1521-0111/12/8201-68–79$25.00
MOLECULAR PHARMACOLOGY
Vol. 82, No. 1
76679/3776766

Mol Pharmacol 82:68–79, 2012

Novel Transcriptome Profiling Analyses Demonstrate that Selective Peroxisome Proliferator-Activated Receptor γ (PPARγ) Modulators Display Attenuated and Selective Gene Regulatory Activity in Comparison with PPARγ Full Agonists[S]

Yejun Tan, Eric S. Muise, Hongyue Dai, Richard Raubertas, Kenny K. Wong, G. Marie Thompson, Harold B. Wood, Peter T. Meinke, Pek Yee Lum, John R. Thompson, and Joel P. Berger

Departments of Informatics and Analysis (Y.T., E.S.M., H.D., P.Y.L., J.R.T.), Early Development Statistics (R.R.), Atherosclerosis (K.K.W.), Diabetes (G.M.T., J.P.B.), and Medicinal Chemistry (H.B.W., P.T.M.), Merck Research Laboratories, Rahway, New Jersey

Received November 2, 2011; accepted April 10, 2012

ABSTRACT

Selective peroxisome proliferator-activated receptor γ (PPARγ) modulators (SPPARγMs) have been actively pursued as the next generation of insulin-sensitizing antidiabetic drugs, because the currently marketed PPARγ full agonists, pioglitazone and rosiglitazone, have been reported to produce serious adverse effects among patients with type 2 diabetes mellitus. We conducted extensive transcriptome profiling studies to characterize and to contrast the activities of 70 SPPARγMs and seven PPARγ full agonists. In both 3T3-L1 adipocytes and adipose tissue from *db*/*db* mice, the SPPARγMs generated attenuated and selective gene-regulatory responses, in comparison with full agonists. More importantly, SPPARγMs regulated the expression of antidiabetic efficacy-associated genes to a greater extent than that of adverse effect-associated genes, whereas PPARγ full agonists regulated both gene sets proportionally. Such SPPARγM selectivity demonstrates that PPARγ ligand regulation of gene expression can be fine-tuned, and not just turned on and off, to achieve precise control of complex cellular and physiological functions. It also provides a potential molecular basis for the superior therapeutic window previously observed with SPPARγMs versus full agonists. On the basis of our profiling results, we introduce two novel, gene expression-based scores, the γ activation index and the selectivity index, to aid in the detection and characterization of novel SPPARγMs. These studies provide new insights into the gene-regulatory activity of SPPARγMs as well as novel quantitative indices to facilitate the identification of PPARγ ligands with robust insulin-sensitizing activity and improved tolerance among patients with type 2 diabetes, compared with presently available PPARγ agonist drugs.

Introduction

The three peroxisome proliferator-activated receptor (PPAR) isoforms, PPARγ, PPARα, and PPARδ, constitute a subclass of the nuclear receptor superfamily of ligand-modulated transcription factors (Willson et al., 2001; Berger and Moller, 2002; Francis et al., 2003). PPARγ is expressed at elevated levels in adipocytes and has been shown to play a central role in regulating adipocyte differentiation, lipid metabolism, glucose homeostasis, and insulin sensitivity (Tontonoz et al., 1994; Schoonjans et al., 1996; Knouff and Auwerx, 2004; Rangwala and Lazar, 2004). Numerous structurally distinct, synthetic, PPARγ ligands have been shown to be insulin-sensitizing agents (Saltiel and Olefsky, 1996; Berger and Moller, 2002; Wang and Tafuri, 2003). Two currently marketed thiazolidinedione (TZD) drugs that have demonstrated notable insulin-

All authors are current or former full-time employees of Merck and Co., Inc. Y.T., J.R.T. and J.P.B. are co-senior authors.

Article, publication date, and citation information can be found at http://molpharm.aspetjournals.org.
http://dx.doi.org/10.1124/mol.111.076679.

[S] The online version of this article (available at http://molpharm.aspetjournals.org) contains supplemental material.

ABBREVIATIONS: PPAR, peroxisome proliferator-activated receptor; EWAT, epididymal white adipose tissue; FABP4, fatty acid binding protein 4; GAI, γ activation index; LBD, ligand binding domain; LXR, liver X receptor; T2D, type 2 diabetes; nTZDpa, nonthiazolidinedione peroxisome proliferator-activated receptor γ partial agonist; SD, Sprague-Dawley; SI, selectivity index; SPPARγM, selective peroxisome proliferator-activated receptor γ modulator; TA, transactivation; TZD, thiazolidinedione; MK-0533, (2*R*)-2-(3-{3-[(4-methoxyphenyl)carbonyl]-2-methyl-6-(trifluoromethoxy)-1*H*-indol-1-yl}phenoxy)butanoic acid; S26948, dimethyl-2-{4-[2-(6-benzoyl-2-oxo-1,3-benzothiazol-3(2*H*)yl)ethoxy]benzyl}malonate; PAR-1622, (*S*)-2-ethoxy-3-[4-(5-[4-[5-(methoxymethylisoxazol-3-yl)phenyl]-3-methylthiophen-2-yl]methoxy)phenyl]propanoic acid.

sensitizing and antihyperglycemic efficacy among patients with type 2 diabetes mellitus, i.e., rosiglitazone and pioglitazone, are PPARγ agonists. Despite their beneficial actions, the use of these compounds has been constrained by their numerous adverse effects, including weight gain, increased adiposity, plasma volume expansion, edema, and an increased risk of congestive heart failure in human subjects, as well as cardiac hypertrophy in a variety of preclinical species (Peraza et al., 2006). As a result of the observed limitations of TZD PPARγ full agonists, the need to identify and to develop novel classes of PPARγ ligands that could provide robust antidiabetic efficacy with diminished untoward effects became apparent.

We previously described nTZDpa, a non-TZD SPPARγM that binds to PPARγ with high affinity and, like PPARγ full agonists, completely displaces a radiolabeled ligand from the receptor in competition binding assays. In contrast to PPARγ full agonists, nTZDpa only partially activates the receptor in cell-based transcriptional activity assays and has a reduced ability to induce maximal 3T3-L1 cell adipogenesis (Berger et al., 2003). Importantly, nTZDpa mitigates insulin resistance and hyperglycemia in obese diabetic rodents to a similar degree, compared with a potent TZD PPARγ full agonist, but without increasing cardiac weight and adiposity, as was observed with the latter ligand. We reported that compounds 24 and 12, two structurally distinct, non-TZD SPPARγMs, are efficacious antihyperglycemic agents in diabetic rodents, with improved therapeutic indices, compared with rosiglitazone, with respect to the induction of cardiomegaly and excessive adiposity (Acton et al., 2005; Liu et al., 2005). In addition, we showed that SPPARγM5, another non-TZD ligand, has notable insulin-sensitizing efficacy and a cardiovascular tolerability profile superior to that of rosiglitazone in obese, insulin-resistant rats (Chang et al., 2008). Numerous other SPPARγMs, including INT131 (structure in Motani et al., 2009), (*S*)-2-ethoxy-3-[4-(5-[4-[5-(methoxymethylisoxazol-3-yl)phenyl]-3-methylthiophen-2-yl]methoxy)phenyl]propanoic acid (PAR-1622) (Kim et al., 2009), (2*R*)-2-(3-{3-[(4-methoxyphenyl)carbonyl]-2-methyl-6-(trifluoromethoxy)-1*H*-indol-1-yl}phenoxy)butanoic acid (MK-0533) (Acton et al., 2009), balaglitazone (Larsen et al., 2008), and dimethyl-2-{4-[2-(6-benzoyl-2-oxo-1,3-benzothiazol-3(2*H*)yl)ethoxy]benzyl}malonate (S26948) (Sohn et al., 2009), have been identified that demonstrate effective insulin sensitization with reduced or no PPARγ-related adverse effects in preclinical species (Zhang et al., 2007; Doshi et al., 2010). These studies support the proposition that SPPARγMs are not simply agonists with diminished maximal activity but are truly selective in their pharmacological actions.

On the basis of extensive pharmacological and genetic experimentation, it is now generally accepted that, because they are effectors of a master transcriptional regulator that is highly expressed in adipocytes, many of the major actions of PPARγ ligands are mediated by their ability to alter gene expression in these cells. A corollary to this theory is that PPARγ ligands that have unique physiological effects should have different adipocyte gene signatures. To test this proposition, we compared the global gene expression signatures of a series of PPARγ full agonists and SPPARγMs in fully differentiated 3T3-L1 adipocytes, a well accepted in vitro model of rodent adipocytes. The results of these studies were extended and fortified by broadly examining changes in gene expression in adipose tissue of mice and rats treated with these PPARγ ligands. The discovery of both common and distinct gene expression patterns between PPARγ full agonists and SPPARγMs furthered our understanding of the molecular basis for their shared efficacy but differential induction of adverse effects. Importantly, such profiling data allowed us to address the fundamental question of whether SPPARγMs are merely weak PPARγ agonists or are truly selective nuclear receptor modulators that demonstrate distinct regulation of gene expression. The knowledge gained through these profiling studies allowed us to develop novel gene expression-based indices that can be used to screen for, to characterize, and to select optimized SPPARγMs with the greatest probability of becoming T2D therapeutic agents with robust efficacy and enhanced tolerability, relative to currently marketed PPARγ agonists.

Materials and Methods

Compounds. SPPARγMs L1 to L20 (Supplemental Table 1), 2-[2-(4-phenoxy-2-propylphenoxy)ethyl]indole-5-acetic acid (COOH) (Carley et al., 2004), TZDfa (Einstein et al., 2008), and LXR agonist 1 were provided by Merck Research Laboratories (Rahway, NJ). PPARα agonist 1 was purchased from Chemsyn (Lenexa, KS). SPPARγM-L2, SPPARγM-L3, SPPARγM-L5, and SPPARγM-L14 were referred to previously as SPPARγM1, SPPARγM2, nTZDpa, and SPPARγM8, respectively (Einstein et al., 2008). SPPARγM-L20 was referred to previously as SPPARγM6 (Acton et al., 2009). Rosiglitazone was used as a bridging compound and was profiled in all batches of profiling experiments.

Cell-Based PPARγ Transactivation and FABP4 Assays. COS-1 cells were cultured and transactivation assays were performed as described previously (Berger et al., 1999). Briefly, cells were transfected with a pcDNA3-hPPARγ/GAL4 expression vector, pUAS(5X)-tk-luc reporter vector, and pCMV-lacZ, as an internal control for transactivation efficiency, by using Lipofectamine (Invitrogen, Carlsbad, CA). After 48-h exposure to compounds, cell lysates were produced, and luciferase and β-galactosidase activities in cell extracts were determined. Inflection points (EC_{50}) of normalized luciferase activity data were calculated with a four-parameter logistic equation.

FABP4 assays were performed as described previously (Thompson et al., 2004). Briefly, 3T3-L1 preadipocyte cells (cell line CL-173; American Type Culture Collection, Manassas, VA) were treated with ligand for 5 days, and FABP4 mRNA expression levels were measured in cell lysates on the basis of hybridization of the mRNA to target-specific oligonucleotides that were conjugated to biotin. Streptavidin-conjugated alkaline phosphatase was then used with the fluorescent alkaline phosphatase substrate StarBright Green Phosphate (Sigma-Aldrich, St. Louis, MO) to quantitate mRNA levels.

3T3-L1 Adipocyte Differentiation and Treatment. 3T3-L1 preadipocyte cells were induced to differentiate fully into adipocytes with a protocol described previously (Gerhold et al., 2002). At day 8, the cells were incubated with vehicle or test ligands for 24 h. Saturating concentrations of ligands were defined as 30 times their EC_{50} values in the cell-based PPARγ transactivation assay described above. Preliminary profiling studies demonstrated that this concentration consistently provided maximal gene-regulatory activity in 3T3-L1 adipocytes with a wide variety of ligands (data not shown).

***db/db* Mouse Studies.** All animal experiments and euthanasia protocols were conducted in accordance with the *Guide for the Care and Use of Laboratory Animals* (Institute of Laboratory Animal Resources (1996)). Animal experiment protocols were reviewed and approved by the Institutional Animal Care and Use Committee of Merck Research Laboratories. The laboratory animal facilities of Merck Research Laboratories have been certified by the Association for Assessment and Accreditation of Laboratory Animal Care Inter-

national. Animals were housed in temperature-, humidity-, and light-controlled rooms (21–23°C, 47–65% humidity, and 12/12-h light/dark cycle, respectively).

Diabetic male *db/db* mice (The Jackson Laboratory, Bar Harbor, ME) with a C57B1/KFJ background, as described previously (Chen et al., 1996; Combs et al., 2002), were given vehicle (0.25% methylcellulose) or test compounds, dosed at approximately 1 times and 3 to 10 times the ED_{50} for glucose level decreases, once daily for 8 days through oral gavage. All animals were euthanized through CO_2 asphyxiation 6 h after the eighth dose, and the epididymal white adipose tissue (EWAT) was harvested and flash-frozen in liquid nitrogen. Serum glucose measurements were taken at the onset (before dosing, denoted as Glu_0) and 24 h after the seventh dose (Glu_7) by using a glucose Trinder assay kit (Sigma-Aldrich). The percentage glucose level correction was computed as 100 − [100 × (*db/db*Drug − LeanVehicle)/(*db/db*Vehicle − LeanVehicle)], by using Glu_7 glucose measurements. The percentage glucose level-lowering was computed as [(Glu_0 − Glu_7)/Glu_0] × 100 for each individually profiled mouse.

Sprague-Dawley Rat Studies. Male Sprague-Dawley (SD) rats (Charles River Laboratories, Wilmington, MA) were treated with the vehicle (0.25% methylcellulose) or test compounds. Animals were given compound once daily for 7 days through oral gavage, at 1, 3, and 10 times the ED_{50} for *db/db* mouse glucose level-lowering. All animals were euthanized through CO_2 asphyxiation approximately 24 h after the seventh dose, and EWAT samples were harvested and flash-frozen in liquid nitrogen. Heart and body weights were measured at the end of the study.

Microarray Profiling. The microarrays used for 3T3-L1 adipocytes and *db/db* mouse profiling experiments were Agilent 25K v1.2 mouse DNA microarrays (Agilent Technologies, Santa Clara, CA), which contain 23,698 probes (reporters), corresponding to 22,775 unique transcripts and 17,192 unique Entrez genes. The microarrays used for the SD rat profiling experiments were Agilent 25K v1.2 rat DNA microarrays, which contain 23,698 probes, corresponding to 22,503 unique transcripts and 11,219 unique Entrez genes. The microarrays we used contained two or three duplicate 60-mer probes targeting different sequence regions for a small proportion of genes. Because the expression associated with each of the duplicate probes was measured independently and the number of genes with duplicate probes was not large enough to change any of our conclusions, we used probe number rather than unique gene number to describe our gene signature results throughout this article.

Total RNA was prepared from the 3T3-L1 adipocytes or EWAT after homogenization by using TRIzol reagent (Invitrogen) with a PT 10/35 Polytron homogenizer (Kinematica, Bohemia, NY) and was processed by using RNeasy kits (QIAGEN, Valencia, CA), according to the manufacturer's instructions; RNA concentrations were estimated from 260-nm absorbance values. Total RNA samples were further processed in the microarray experiments as reported previously (Hughes et al., 2001). Labeled cRNA was hybridized for 48 h on Agilent 60-mer, two-color, spotted microarrays. Individual samples from vehicle and test compound treatments were hybridized against a reference pool composed of an equal amount of cRNA from the vehicle treatment samples. Fluor-reversed pairs were constructed for each individual comparison.

Analytical Methods for Profiling Data. The raw microarray data were processed with Rosetta Resolver (Rosetta Biosoftware, Seattle, WA) and MatLab (MathWorks, Natick, MA) software by using the Rosetta error model (Weng et al., 2006). Differences in expression were quantified as the ratio between normalized, background-corrected, intensity values for the two channels (red and green) for each spot on the array and were expressed as either log ratio ($\log_{10}$ of the ratio) or fold change (the ratio itself when it was ≥1.0 and the reciprocal of the ratio otherwise) values. Data from replicates (i.e., multiple samples in the same treatment group) were weighted and combined by using an error model (Weng et al., 2006), to quantify the significance of expression changes between the test compound and vehicle treatments. For Fig. 1, signature genes were defined as those with error-weighted, replicate-combined, p values of <0.01 and fold change values of >1.5 for any test compound, with masking of genes with strong signals in the vehicle group. The latter genes were defined as genes with error-weighted, replicate-combined, p values of <0.01 in the vehicle group or genes with p values of <0.01 for each of the three individual vehicle self-references. Additional statistical analyses are specified in the figure legends. The expression data were uploaded to the Gene Expression Omnibus database (accession number GSE31222).

PPAR γ Activation Index. The statistical approach used to compute the PPAR γ activation index (GAI), S, for a test compound was χ^2 fitting, in which S was selected to minimize the function $\chi^2 = \Sigma[(SX_i - Y_i)^2/(\sigma^2_{Xi} + \sigma^2_{Yi})]$, where X_i and σ_{Xi} indicate the log ratio and its error, respectively, for the ith gene for the reference compound (here, rosiglitazone) and Y_i and σ_{Yi} indicate the log ratio and its error, respectively, for the test compound. S is the slope from a weighted, least-squares fit of a through-the-origin line to log ratio data for the reference and test compounds. For compounds with replicate profiles, the combined GAI scores were obtained by averaging values within a batch and then averaging values across batches if the compound was profiled in more than one batch.

The probes used in the fitting were selected for their ability to discriminate between PPARγ full agonists and SPPARγMs. The selection was performed by applying t tests to a training set consisting of profiles for two PPARγ full agonists (total of six profiles) and four SPPARγMs (total of 12 profiles) in 3T3-L1 adipocytes. The 303 selected probes resulted from application of a threshold of $p < 10^{-7}$ to the comparison of full agonists with SPPARγMs and an averaged fold change for the two PPARγ full agonists of >1.5, relative to vehicle. The accession codes, gene symbols, probe identifications, and probe sequences for the selected 303 probes are provided in Supplemental Table 2.

Antidiabetic Efficacy-Associated Gene Set and Adverse Effect-Associated Gene Set. The antidiabetic efficacy-associated gene set was obtained from *db/db* mouse EWAT profiling experiments through the following steps. First, genes with expression levels that significantly correlated ($p < 0.01$) with the efficacy endpoint data (glucose level correction) were selected and then intersected with genes that exhibited robust regulation by PPARγ full agonists ($p < 0.01$ for the error-weighted, replicate-combined, log ratio and fold change of >1.2 in at least two of four high-dose PPARγ full agonist treatment groups and $p < 0.01$ and fold change of >1.3 in the 100 mg/kg rosiglitazone treatment group). A total of 610 probes were obtained through the selection. Second, a fullness score (F_i) was determined for each individually profiled animal i by using rosiglitazone at 100 mg/kg as the reference in the same χ^2 fitting procedure as for the GAI score but using the 610 probes from step 1 instead of the 303. Third, the ratio G_i was computed by dividing the glucose level correction for animal i by the average glucose level correction for animals with 100 mg/kg rosiglitazone treatment. Fourth, the ratio R_{ij} was calculated by dividing the log ratio of probe j with animal i by the average log ratio of probe j with animals treated with 100 mg/kg rosiglitazone. Fifth, mice that were treated with SPPARγMs and displayed F_i values of >0.3 were preselected, and then probes with R_{ij} values greater than F_i for >80% of the preselected animals were selected. Sixth, mice that were treated with SPPARγMs and displayed glucose level correction values of >40% and glucose level-lowering values of >40% were preselected, and then probes with R_{ij} values greater than G_i for >60% of the preselected animals were selected. Seventh, 29 probes were obtained by intersecting the genes identified in steps 1, 5, and 6 above and were named the antidiabetic efficacy-associated genes.

A similar approach was applied to the SD rat profiling experiments to select the adverse effect-associated genes, by using EWAT RNA profiles and heart weight normalized by body weight as the endpoint. First, 358 probes were selected from the correlation analysis of EWAT

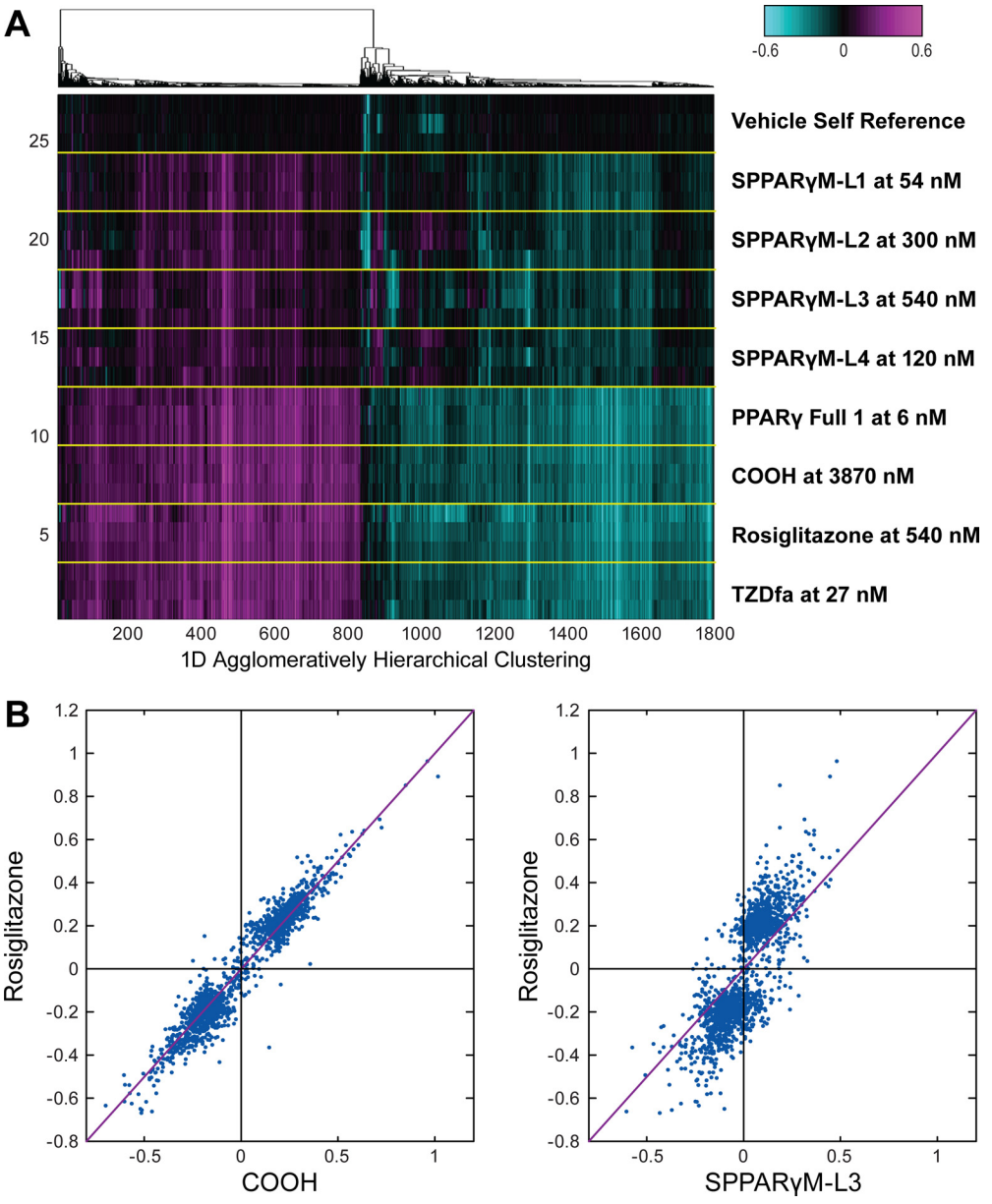

Fig. 1. PPARγ ligand-induced 3T3-L1 adipocyte gene expression signatures. A, one-dimensional agglomerative clustering of gene expression data from 3T3-L1 adipocytes treated with four PPARγ full agonists [PPARγ full 1, COOH, rosiglitazone, and TZD full agonist (TZDfa)] and four SPPARγMs (L1–L4). Each compound treatment group contains three fluor-reversed pairs in which an individual sample was hybridized against a vehicle treatment reference pool. Each compound was dosed at 30 times its EC_{50} value in an in vitro PPARγ transactivation assay. Shown are log ratio values. The magenta color denotes genes that were up-regulated by the ligands, compared with vehicle; the cyan color indicates genes that were down-regulated. Shown are 1812 probes that met the criteria of a p value of <0.01 and a 1.5-fold change for at least one of the eight compounds. B, log ratios for rosiglitazone versus COOH (left) and rosiglitazone versus SPPARγM-L3 (right), for the same 1812 probes as in A.

gene expression with the normalized heart weight endpoint. Second, F_i was computed for each individually profiled animal i by using the same χ^2 fitting method as described above. Third, the ratio W_i was calculated by dividing the normalized heart weight endpoint for animal i by the average normalized heart weight endpoint for animals treated with 100 mg/kg rosiglitazone. Fourth, the ratio R_{ij} was determined by dividing the log ratio of probe j for animal i by the average log ratio of probe j for animals treated with 100 mg/kg rosiglitazone. Fifth, rats that were treated with SPPARγMs and had F_i values of >0.2 were preselected, and then genes with R_{ij} values greater than 0 and less than F_i for $\geq 60\%$ of the preselected animals were selected. Sixth, rats that were treated with SPPARγMs and had normalized heart weights of >0.0032 were preselected, and then genes with R_{ij} values greater than 0 and less than 50% of W_i for $\geq 80\%$ of the preselected animals were selected. Seventh, the intersecting genes identified from steps 1, 5, and 6 above were mapped to homologous genes on mouse microarrays. Nineteen probes were obtained through this process and were named the adverse effect-associated genes. The accession codes, gene symbols, probe identifications, and probe sequences for the selected 29 and 19 probes are provided in Supplemental Tables 3 and 4, respectively.

Antidiabetic Efficacy-Associated Gene Score, Adverse Effect-Associated Gene Score, and Selectivity Index. The antidiabetic efficacy-associated gene score and the adverse effect-associated gene score were computed through the same method as described for the GAI score but using the aforementioned 29 and 19 selected probes, respectively. The SPPARγM selectivity index (SI) was obtained by subtracting the adverse effect-associated gene score from the antidiabetic efficacy-associated gene score and then dividing the result by the square root of 2. The SI is equal to the distance of each dot from the 45° line in Fig. 5, A and B.

Pathway Enrichment Analysis. Enrichment of Gene Ontology Biological Process terms in the annotation of sets of probes was tested by using Gene Set Annotator in the Merck Target and Gene Information System, which provides pathway enrichment analysis to identify gene sets in which a user-supplied set of identifiers is significantly enriched. The p values were calculated by using the hypergeometric distribution and the E values from the Bonferroni-adjusted p values. Gene overlap was based on mouse database identifications. The allowed maximal and minimal gene set sizes for the pathway terms were 500 and 5, respectively.

Results

SPPARγMs Produce Attenuated 3T3-L1 Adipocyte Gene Signatures, Compared with PPARγ Full Agonists. To examine the effects of different PPARγ ligands on global gene expression, we began by incubating 3T3-L1 adipocytes with four PPARγ full agonists and four SPPARγMs (Table 1) at saturating concentrations for 24 h. The cells were then harvested and their transcriptomes were profiled with Agilent mouse 25K custom arrays. A one-dimensional agglomerative clustergram of genes affected by any of the PPARγ full agonists or SPPARγMs is shown in Fig. 1A. The 1812 probes within the clustergram were selected by using a threshold of an error-weighted, replicate-combined, p value of <0.01 and a fold change of >1.5 for any compound. The PPARγ full agonists produced robust and highly similar gene signatures both for replicate samples for each compound and for structurally distinct compounds. For example, PPARγ full agonist 1 and COOH are non-TZDs, but their signatures were indistinguishable from those of the TZD full agonists rosiglitazone and TZD full agonist (Fig. 1A). No robust, consistent, SPPARγM-specific effects on gene expression were observed. Notably, the SPPARγMs displayed similar but attenuated gene regulation patterns, compared with the PPARγ full agonists (Fig. 1A). Qualitatively, the SPPARγM-induced signatures seemed to be a subset of those generated by the PPARγ full agonists.

TABLE 1
Names and structures of PPARγ full agonists and SPPARγMs profiled in Fig. 1

Compound	Structure
SPPARγM-L1	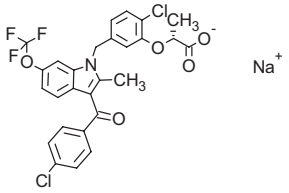
SPPARγM-L2	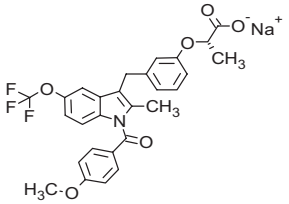
SPPARγM-L3	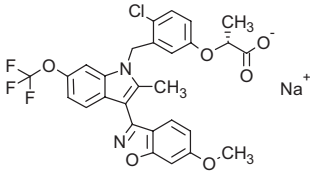
SPPARγM-L4	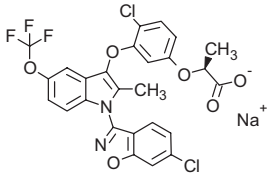
PPARγ Full 1	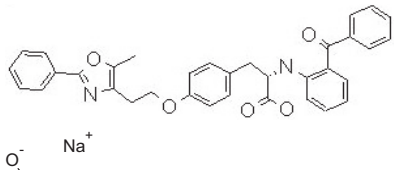
COOH	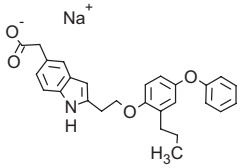
Rosiglitazone	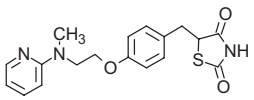

To examine the gene-regulating activities of three distinct representative ligands in a different manner, we compared the expression log ratios (error-weighted averages of three replicates) of the 1812 probes for rosiglitazone versus the non-TZD PPARγ full agonist COOH and SPPARγM-L3 (Fig. 1B). In Fig. 1B, left, the genes were generally distributed along a 45° line, which indicated that they were regulated similarly by the TZD and non-TZD PPARγ full agonists. In Fig. 1B, right, however, the gene expression changes were shifted counterclockwise from the 45° diagonal line, which indicated that SPPARγM-L3 produced an attenuated gene-modulatory response, compared with rosiglitazone. Similar plots for the other SPPARγMs that were profiled were essentially identical (data not shown), which supports the conclusion that, in 3T3-L1 adipocytes, SPPARγMs produced analogous but attenuated gene signatures, compared with PPARγ full agonists.

SPPARγM 3T3-L1 Adipocyte Signatures Are Dominated by Genes Involved in Numerous Metabolic Pathways. We next examined and compared the gene signatures of PPARγ full agonists and SPPARγMs. Figure 2 is a representative, three-way, Venn diagram of the signature genes for two full agonists (rosiglitazone and COOH) and SPPARγM-L3. The values shown are the number of probes that were significantly regulated in 3T3-L1 adipocytes by the respective compounds, compared with the vehicle reference pool (error-weighted, replicate-combined, p value of <0.01 and fold change of >1.5). With such selection criteria, the SPPARγM-L3 signature had a total of 367 probes, whereas the rosiglitazone and COOH signatures had totals of 1469 and 1786 probes, respectively. The intersection of the three signature sets was found to contain 318 probes; these 318 probes represented 293 unique genes. The 318 overlapping probes constituted 86.6% of the SPPARγM-L3 signa-

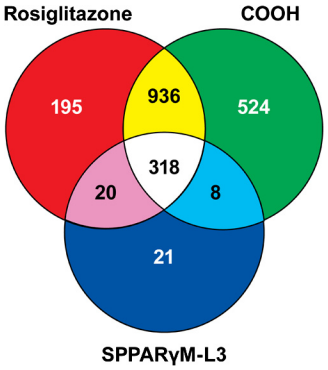

Fig. 2. Venn diagram of 3T3-L1 adipocyte signature genes generated with two PPARγ full agonists and a SPPARγM. The gene sets for rosiglitazone (top left), COOH (top right), and SPPARγM-L3 (bottom) used to generate the diagram had p values of <0.01 and 1.5-fold changes, compared with vehicle, as shown in Table 2.

tures but only 21.7% and 17.8% of the rosiglitazone and COOH signatures, respectively (Table 2). The same observation holds true regardless of the fold-change threshold used as the basis of comparison, as well as for other SPPARγMs that we profiled in a similar manner (data not shown).

Given that PPARγ full agonists and SPPARγMs bind and activate the same nuclear receptor and have been shown to possess comparable glucose-lowering and insulin-sensitizing efficacies (Berger et al., 2003; Chang et al., 2008), we thought it probable that the overlapping genes would be associated with the ligands' common beneficial effects on nutrient metabolism and would be enriched in metabolic pathway functions. To test this hypothesis, we conducted Gene Ontology Biological Process term-enrichment analysis, by using Gene Set Annotator in the Merck Target and Gene Information System, for the 318 probes common to the signatures of all three compounds in Fig. 2. Table 3 shows the top 50 terms that were enriched in this probe set (hypergeometric $p < 0.002$). Twenty-two of the top terms are related to nutrient metabolism, including pyruvate, acetyl-CoA, and lipid metabolism and insulin signaling. Several important lipid and glucose metabolism-regulatory genes with bona fide peroxisome proliferator response elements in their promoters, such as FABP4, phosphoenolpyruvate carboxykinase, acyl-CoA oxidase, and pyruvate dehydrogenase kinase 4, were found within the common signature. In contrast, the top 50 pathways from the enrichment analysis for the 936 probes common to the gene signatures for the two PPARγ full agonists but not for SPPARγM-L3 contained fewer metabolic pathway terms. The fact that many of the top-ranked terms for these 936 probes were related to apoptosis and blood vessel development may provide some mechanistic clues to the findings regarding hemangiomas/hemangiosarcomas or other cancers observed in 2-year, high-dose, preclinical, safety-assessment studies with some PPARγ full agonists and PPAR dual agonists (Center for Drug Evaluation and Research, 2008; Doshi et al., 2010).

A Novel Gene Expression Score Can Differentiate SPPARγMs from PPARγ Full Agonists Profiled at Saturating Doses. One important question we sought to answer was whether the 3T3-L1 adipocyte gene expression profiles obtained with saturating ligand doses could be used to distinguish quantitatively SPPARγMs from PPARγ full agonists and from non-PPARγ ligands. A small group of ligand profiles was used as a training set to select genes to build a classifier, and a separate larger group was used as a testing set to evaluate the performance of the classifier. The training set consisted of profiles for saturating concentrations of two PPARγ full agonists and four SPPARγMs, whereas the testing set consisted of 29 independent compound profiles, including five PPARγ full agonists, 21 SPPARγMs, two PPARα agonists, and one LXR agonist.

Analysis of variance, applied separately to each probe in the PPARγ ligand gene signatures, identified 303 probes that could best discriminate PPARγ full agonists from SPPARγMs in the training set. These 303 probes corresponded to 291 unique genes. The magnitude of changes in the expression of these probes induced by a given ligand were consolidated into a single score by fitting a line relating the log ratio for the ligand to the log ratio for the reference compound, rosiglitazone, as described in *Materials and Methods*. This score was named the PPAR GAI. Figure 3A is an expression heatmap of the 303 GAI probes for all training and testing ligand profiles. The dot plot on the right shows the GAI score for each ligand treatment. When the ligands were sorted on the basis of their GAI scores, all of the PPARγ full agonists clustered together below the blue line, whereas all of the SPPARγMs clustered above it. The profiles of an LXR agonist and two PPARα agonists at the top of Fig. 3A indicated that they had little impact on the expression of the 303 probes, in line with the expectation that such ligands would not act as PPARγ activators and could serve as useful negative controls.

The GAI is a statistically derived score that can be used to report the degree of gene regulation induced by a PPARγ ligand. The GAI is a relative score, in that each compound is compared with a reference compound (in this case, rosiglitazone). Figure 3B contains the replicate-combined GAI scores for 79 profiled ligands, including 70 SPPARγMs, 7 PPARγ full agonists, 1 PPARα agonist, and 1 LXR agonist. The ligands were all tested at saturating concentrations, to ensure that they were providing their maximal transcriptional activity. The GAI scores ranged from 0 to 1. The greater the maximal transcriptional activity of a PPARγ ligand was, the higher its GAI score was. For TZD and non-TZD PPARγ full agonists, GAI scores were >0.95. In contrast, GAI scores for the various SPPARγMs ranged from 0.2 to 0.82, reflecting a wide range of partial receptor activation. PPARα and LXR agonists had scores of <0.1.

GAI scores for individual ligands were highly reproducible within and across different batches of profiling experiments. In general, the S.D. was <0.05 and the coefficient of variation was approximately 5 to 10%. The GAI scores for all of the ligands we tested were compared with the maximal activities they demonstrated in PPARγ transactivation (TA) (Fig. 4A) and FABP4 expression (Fig. 4B) assays. These two cell-based assays were used previously to characterize the functional activity of PPARγ ligands (Berger et al., 1999, 2003; Thompson et al., 2004). The overall Pearson correlation coefficient for correlation between the GAI and TA scores was 0.85 ($p = 1.9 \times 10^{-22}$). The correlation between GAI and FABP4 scores

TABLE 2
Numbers of overlapping and total probes in signatures obtained with different fold change cutoff values

Fold Change Cutoff Value	No. of Overlaps	No. of Probes in Total Signature			Overlaps/Total Signature		
		Rosiglitazone	COOH	SPPARγM-L3	Rosiglitazone	COOH	SPPARγM-L3
						%	
1.0	2831	5475	6450	3894	51.71	43.89	72.70
1.2	1867	4469	5164	2447	41.78	36.15	76.30
1.3	943	3041	3567	1192	31.01	26.44	79.11
1.5	318	1469	1786	367	21.65	17.81	86.65
1.8	67	608	769	78	11.02	8.71	85.90
2.0	38	367	449	43	10.35	8.46	88.37

TABLE 3

Top 50 Gene Ontology Biological Process terms enriched in 318- and 936-probe sets through three-way intersection of rosiglitazone, COOH, and SPPARγM-L3 gene signatures

Genes in the three signatures demonstrated fold changes of >1.5 with p values of <0.01. The transcript names and gene symbols for the overlapping genes in the Gene Ontology Biological Process analysis are provided in Supplemental Tables 5 and 6.

Rank	318-Probe Set			936-Probe Set		
	Term	Hypergeometric p	Bonferroni-Adjusted p	Term	Hypergeometric p	Bonferroni-Adjusted p
1	Response to osmotic stress	2.58×10^{-7}	4.84×10^{-4}	Energy pathways[a]	0.00	0.00
2	Alcohol metabolism[a]	2.78×10^{-7}	5.21×10^{-4}	Positive regulation of programmed cell death	1.46×10^{-12}	2.74×10^{-9}
3	Angiogenesis	5.58×10^{-7}	1.05×10^{-3}	Positive regulation of apoptosis	1.23×10^{-11}	2.30×10^{-8}
4	Pyruvate metabolism[a]	8.95×10^{-7}	1.68×10^{-3}	Growth	1.16×10^{-10}	2.18×10^{-7}
5	Blood vessel development	1.13×10^{-6}	2.11×10^{-3}	Regulation of cell size	2.12×10^{-10}	3.98×10^{-7}
6	Sterol biosynthesis[a]	1.33×10^{-6}	2.49×10^{-3}	Skeletal development	3.43×10^{-10}	6.44×10^{-7}
7	Sterol metabolism[a]	9.87×10^{-6}	1.85×10^{-2}	Cell growth	3.94×10^{-10}	7.38×10^{-7}
8	Lipid biosynthesis[a]	1.62×10^{-5}	3.03×10^{-2}	Blood vessel development	1.17×10^{-9}	2.19×10^{-6}
9	Cholesterol biosynthesis[a]	2.01×10^{-5}	3.77×10^{-2}	Adipocyte differentiation	1.40×10^{-9}	2.63×10^{-6}
10	Steroid metabolism[a]	2.09×10^{-5}	3.92×10^{-2}	Regulation of development	5.05×10^{-9}	1.10×10^{-5}
11	Fatty acid metabolism[a]	2.21×10^{-5}	4.13×10^{-2}	Induction of apoptosis	1.07×10^{-8}	2.01×10^{-5}
12	Response to hypoxia	3.22×10^{-5}	6.04×10^{-2}	Induction of programmed cell death	1.15×10^{-8}	2.16×10^{-5}
13	Regulation of angiogenesis	5.34×10^{-5}	1.00×10^{-1}	Fatty acid metabolism[a]	3.25×10^{-8}	6.10×10^{-5}
14	Response to inorganic substance	6.09×10^{-5}	1.14×10^{-1}	Angiogenesis	4.53×10^{-8}	8.50×10^{-5}
15	Acetyl-CoA biosynthesis[a]	9.14×10^{-5}	1.71×10^{-1}	Mitotic cell cycle	6.27×10^{-8}	1.18×10^{-4}
16	Response to oxidative stress	9.20×10^{-5}	1.72×10^{-1}	Regulation of growth	2.22×10^{-7}	4.15×10^{-4}
17	Steroid biosynthesis[a]	1.11×10^{-4}	2.08×10^{-1}	Antiapoptosis	3.16×10^{-7}	5.93×10^{-4}
18	Glycerolipid metabolism[a]	1.23×10^{-4}	2.30×10^{-1}	Alcohol metabolism[a]	5.65×10^{-7}	1.06×10^{-3}
19	Defense response to pathogenic fungi	1.25×10^{-4}	2.34×10^{-1}	Negative regulation of apoptosis	6.47×10^{-7}	1.21×10^{-3}
20	Muscle development	1.26×10^{-4}	2.36×10^{-1}	Negative regulation of programmed cell death	7.20×10^{-7}	1.35×10^{-3}
21	Defense response to pathogen	1.46×10^{-4}	2.73×10^{-1}	Actin cytoskeleton organization and biogenesis	1.26×10^{-6}	2.37×10^{-3}
22	Second-messenger-mediated signaling	1.69×10^{-4}	3.16×10^{-1}	Regulation of cell growth	1.30×10^{-6}	2.44×10^{-3}
23	Isoprenoid biosynthesis[a]	2.13×10^{-4}	4.00×10^{-1}	Lipid transport[a]	1.36×10^{-6}	2.54×10^{-3}
24	Cholesterol metabolism[a]	2.39×10^{-4}	4.49×10^{-1}	Regulation of cell migration	1.69×10^{-6}	3.16×10^{-3}
25	Acetyl-CoA metabolism[a]	2.70×10^{-4}	5.06×10^{-1}	Main pathways of carbohydrate metabolism[a]	2.37×10^{-6}	4.45×10^{-3}
26	Lymphocyte proliferation	3.10×10^{-4}	5.80×10^{-1}	Energy derivation by oxidation of organic compounds	3.32×10^{-6}	6.22×10^{-3}
27	Oxygen and reactive oxygen species metabolism	3.18×10^{-4}	5.96×10^{-1}	Tricarboxylic acid cycle[a]	3.53×10^{-6}	6.62×10^{-3}
28	Fatty acid oxidation[a]	3.29×10^{-4}	6.17×10^{-1}	Actin filament-based process	3.65×10^{-6}	6.83×10^{-3}
29	Heart development	3.80×10^{-4}	7.11×10^{-1}	Bone remodeling	5.61×10^{-6}	1.05×10^{-2}
30	Triacylglycerol metabolism[a]	4.69×10^{-4}	8.79×10^{-1}	Ossification	6.05×10^{-6}	1.13×10^{-2}
31	Response to metal ions	4.69×10^{-4}	8.79×10^{-1}	Electron transport[a]	6.76×10^{-6}	1.27×10^{-2}
32	Neuropeptide signaling pathway	5.09×10^{-4}	9.55×10^{-1}	Response to radiation	7.60×10^{-6}	1.42×10^{-2}
33	Defense response to fungi	6.94×10^{-4}	1.30	Cell matrix adhesion	8.32×10^{-6}	1.56×10^{-2}
34	Response to pathogenic fungi	1.08×10^{-3}	2.02	Positive regulation of development	1.23×10^{-5}	2.31×10^{-2}
35	Fatty acid β-oxidation[a]	1.12×10^{-3}	2.10	Extracellular matrix organization and biogenesis	1.72×10^{-5}	3.23×10^{-2}
36	Xenobiotic metabolism	1.15×10^{-3}	2.15	Extracellular structure organization and biogenesis	1.86×10^{-5}	3.49×10^{-2}
37	Excretion	1.15×10^{-3}	2.15	DNA replication and chromosome cycle	1.90×10^{-5}	3.57×10^{-2}
38	Response to pathogenic bacteria	1.25×10^{-3}	2.34	Cholesterol transport[a]	2.25×10^{-5}	4.22×10^{-2}
39	Response to toxin	1.27×10^{-3}	2.39	Reproductive physiological process	2.93×10^{-5}	5.48×10^{-2}
40	Acylglycerol metabolism[a]	1.31×10^{-3}	2.45	Steroid metabolism[a]	3.02×10^{-5}	5.67×10^{-2}
41	Negative regulation of apoptosis	1.40×10^{-3}	2.62	Heart development	3.09×10^{-5}	5.78×10^{-2}
42	Glycerol ether metabolism[a]	1.40×10^{-3}	2.63	Regulation of cell shape	3.88×10^{-5}	7.27×10^{-2}
43	Negative regulation of programmed cell death	1.45×10^{-3}	2.73	Amine metabolism[a]	4.37×10^{-5}	8.18×10^{-2}
44	Neutral lipid metabolism[a]	1.62×10^{-3}	3.03	M phase of mitotic cell cycle	4.54×10^{-5}	8.50×10^{-2}
45	Hyperosmotic response	1.77×10^{-3}	3.32	Pregnancy	5.51×10^{-5}	1.03×10^{-1}
46	Response to cold	1.77×10^{-3}	3.32	M phase-specific microtubule process	5.76×10^{-5}	1.08×10^{-1}
47	Negative regulation of cell adhesion	1.77×10^{-3}	3.32	Positive regulation of body size	6.46×10^{-5}	1.21×10^{-1}
48	Sulfur metabolism	1.89×10^{-3}	3.54	Fatty acid β-oxidation[a]	7.08×10^{-5}	1.33×10^{-1}
49	Isoprenoid metabolism[a]	1.98×10^{-3}	3.70	Pyruvate metabolism[a]	7.56×10^{-5}	1.42×10^{-1}
50	Insulin receptor signaling pathway[a]	1.98×10^{-3}	3.71	Sterol transport	7.59×10^{-5}	1.42×10^{-1}

[a] Direct metabolic pathway.

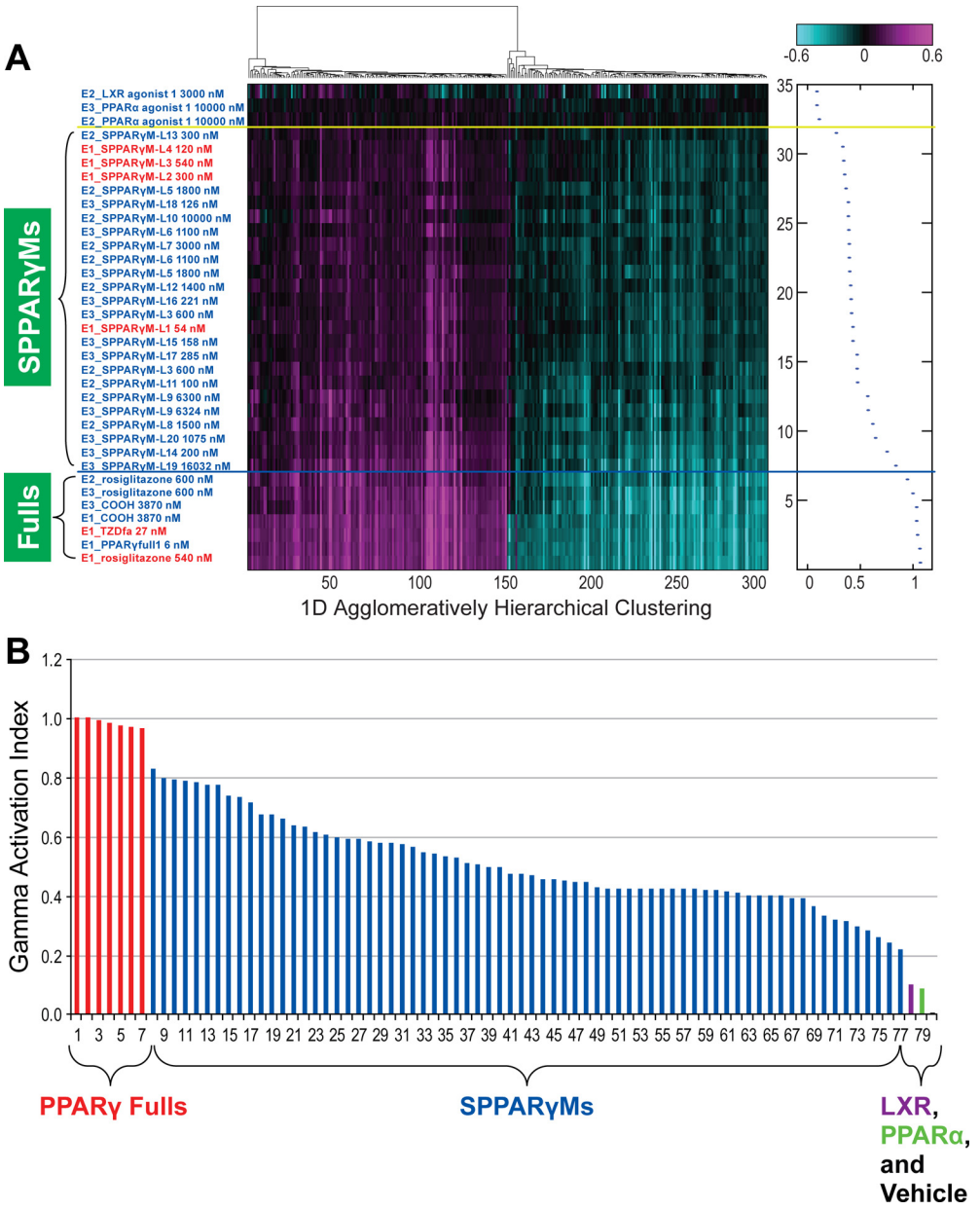

Fig. 3. PPARγ ligand regulation of GAI genes and resulting GAI scores. A, regulation of expression of the 303 GAI probes in 3T3-L1 adipocytes with the training (red) and testing (blue) ligands. The dot plot on the right shows the GAI score for each ligand treatment. The blue line separates the ligands into PPARγ full agonists and SPPARγMs. The yellow line separates PPARγ ligands from non-PPARγ ligands. The profiles were generated in three independent batches of experiments, denoted E1, E2, and E3. Log ratio values are shown with the same color scheme as in the heatmap in Fig. 1. B, replicate-combined GAI scores for seven PPARγ full agonists (red) and 70 SPPARγMs (blue) profiled in 3T3-L1 adipocytes. The three bars at the far right are the scores for LXR agonist 1 (purple), PPARα agonist 1 (green), and vehicle control (black).

was much weaker, with a correlation coefficient equal to 0.4. The correlation between TA scores and FABP4 scores demonstrated a coefficient of 0.31 (data not shown), smaller than the coefficients for the correlation of GAI and TA scores and the correlation of GAI and FABP4 scores.

SPPARγMs Differ from Submaximally Dosed PPARγ Full Agonists in Their Greater Regulation of Antidiabetic Efficacy-Associated Genes versus Adverse Effect-Associated Genes. A key question regarding SPPARγMs that arises from the studies described above is whether they are merely PPARγ partial agonists with decreased maximal activity or are truly "selective" gene modulators that can be differentiated from submaximally dosed PPARγ full agonists on the basis of their distinctive gene expression profiles. We identified two gene sets to address this question. As described in *Materials and Methods*, the first set (29 probes) was derived from *db/db* mouse experiments in which the gene-regulating and glucose-lowering activities of various PPARγ ligands, administered at 1 and 3 times their antihyperglycemic ED_{50} values, were examined. The second gene set (19 probes) was obtained from experiments using SD rats in which the effects of PPARγ ligands, administered at up to 10 times the *db/db* mouse antihyperglycemic ED_{50} values, on gene expression and cardiac hypertrophy were assessed. An antidiabetic efficacy-associated gene score and an adverse effect-associated gene score for a PPARγ ligand could then be computed with the line-fitting approach used for the GAI, with expression data from the aforementioned 29 and 19 probes, respectively. Figure 5A provides a comparison of these two gene scores in a representative, independent, *db/db* mouse EWAT, gene expression profiling experiment for three PPARγ full agonists and three SPPARγMs. All ligands except rosiglitazone were different from those profiled in the *db/db* data set used to select the aforementioned probes. The scores for the PPARγ full agonists, which were tested over a range of doses, generally fell along the 45° line, which indicated that those ligands increased efficacy and adverse effect gene expression proportionally with dose. However, the scores for

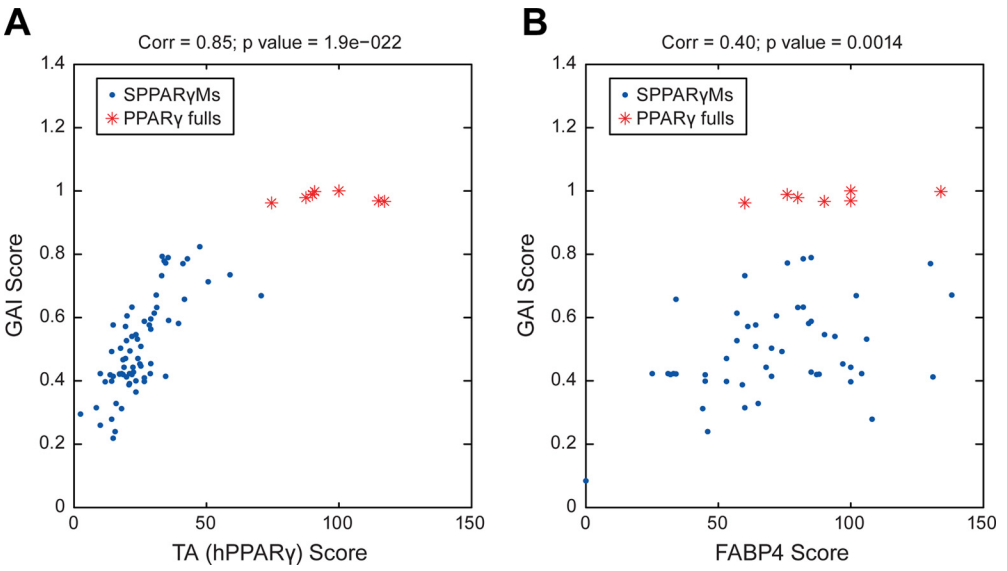

Fig. 4. Comparison of GAI scores versus cell-based TA (A) and FABP4 (B) assay scores for seven PPARγ full agonists (red) and 70 SPPARγMs (blue) that were profiled in 3T3-L1 experiments from batches E1 to E10. All scores are referenced to rosiglitazone. Both TA and FABP4 assay scores are in percentages (22 compounds did not have FABP4 assay data). Corr, correlation coefficient.

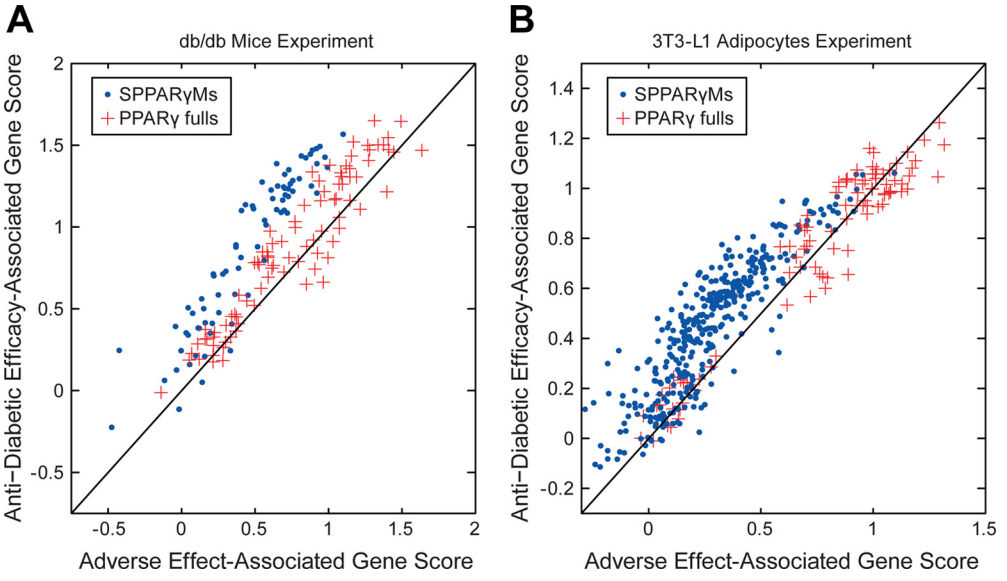

Fig. 5. Comparison of PPARγ ligand gene scores derived from the expression of 29 antidiabetic efficacy-associated probes and 19 adverse effect-associated probes. A, *db/db* mouse EWAT profiling data. Each data point represents one *db/db* animal treated with a PPARγ ligand at a particular dose level. The in vivo profiling experiments shown consisted of treatments with three PPARγ full agonists and three SPPARγMs. B, 3T3-L1 adipocyte profiling data. Each data point represents one 3T3-L1 adipocyte sample treated with a PPARγ ligand at a particular dose level. The experiments shown included treatments with seven PPARγ full agonists and 70 SPPARγMs from batches E1 to E10.

the SPPARγMs were largely well above those for the full agonists. These data demonstrated that, unlike PPARγ full agonists, SPPARγMs did not alter the expression of the two gene sets proportionally but preferentially regulated the antidiabetic efficacy-associated genes to a greater extent than the adverse effect-associated genes.

The selectivity of SPPARγMs relative to PPARγ full agonists was verified by using scores calculated with the same 29- and 19-probe sets in the 10 independent batches of 3T3-L1 adipocyte profiling experiments described above, which used seven PPARγ full agonists and 70 SPPARγMs treatments. It was found that PPARγ full agonists regulated the expression of both gene sets proportionally from low to intermediate to high doses, whereas SPPARγMs altered the expression of the antidiabetic efficacy-associated genes to a greater extent than the adverse effect-associated genes (Fig. 5B). SPPARγMs were once again found almost exclusively above PPARγ full agonists in the 3T3-L1 adipocyte comparison plot.

Another novel gene expression-based score, the SPPARγM SI, was computed from the relative difference between the antidiabetic efficacy-associated gene score and the adverse effect-associated gene score, as described in *Materials and Methods*. The SI scores for all seven PPARγ full agonists and 70 SPPARγMs profiled in 3T3-L1 adipocytes are presented in Fig. 6. The vast majority of SPPARγMs had SI scores above 0, which indicates that they regulated the expression of the antidiabetic efficacy-associated genes to a greater extent than the adverse effect-associated genes. In contrast, the seven profiled PPARγ full agonists generally had SI scores near or below 0, which indicates that they did not possess the same desirable selectivity as was observed for the SPPARγMs. The SI scores for LXR and PPARα ligands were also close to 0.

Unlike the GAI, the SI describes the relative change in expression between two gene sets; it does not depend on ligand dose. We used the SI scores to build a classifier (details not shown) to separate SPPARγMs from submaximally dosed PPARγ full agonists, and we tested its performance with a subset of the independent, *db/db* mouse EWAT, gene profiling experiments. Among 38 blinded samples assayed, the SI classifier correctly identified 16 of 19 animals that

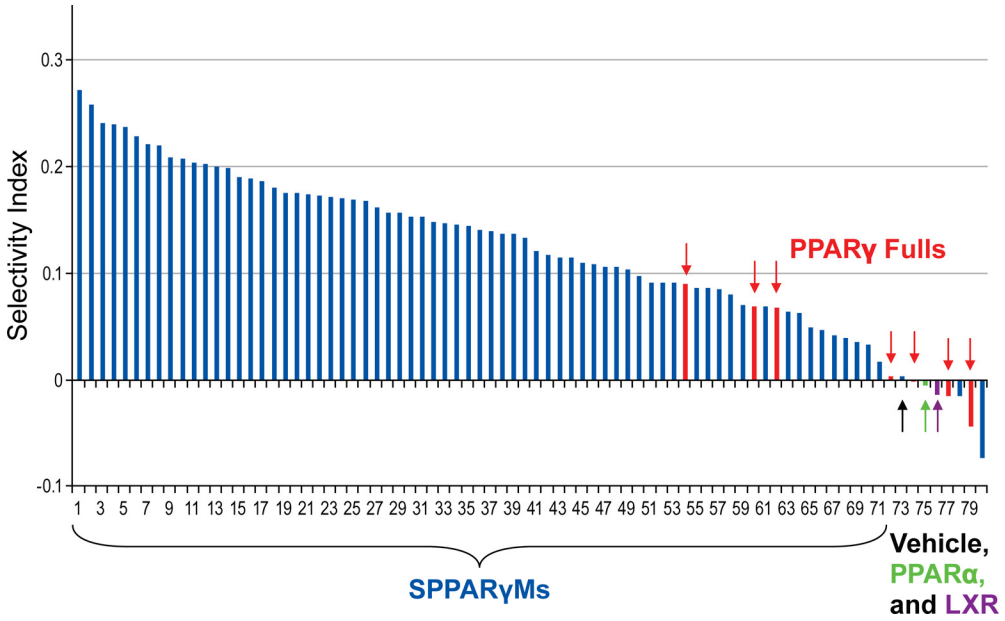

Fig. 6. SI scores for seven PPARγ full agonists (red), 70 SPPARγMs (blue), vehicle control (black), PPARα agonist 1 (green), and LXR agonist 1 (purple). The ligands scored in Fig. 6 and Fig. 3B are from the same data sets but sorted differently, according to the magnitude of SI and GAI scores, respectively.

received submaximal doses of PPARγ full agonists and 18 of 19 animals that were treated with SPPARγMs, which indicates a classification accuracy rate of 90%.

Taken together, these data indicate that, in contrast to PPARγ full agonists, SPPARγMs preferentially regulate antidiabetic efficacy-associated versus adverse effect-associated adipocyte genes. SPPARγMs, although consistently inducing attenuated gene signatures, are not simply weak PPARγ agonists but are selective modulators of PPARγ gene-regulatory activity.

Discussion

We profiled a large set of PPARγ full agonists and SPPARγMs in multiple batches of experiments, both in vitro and in vivo. In 3T3-L1 adipocyte profiling studies, we did not find robust consistent gene signatures that were oppositely regulated by PPARγ full agonists versus multiple SPPARγMs. Similar findings were obtained in in vivo profiling studies using *db/db* mice and SD rats. Instead, we found that saturating concentrations of SPPARγMs produced largely similar but attenuated adipocyte gene signatures, compared with PPARγ full agonists. This attenuation was characterized by fewer significantly regulated genes and an overall smaller magnitude of regulation of genes that demonstrated significantly altered expression.

The gene expression profiles we observed could be summarized by a single score, the GAI, which was used to quantify and to rank the maximal gene-regulatory activity of PPARγ ligands. When GAI scores for a group of ligands were compared with results obtained from two other cell-based, functional assays previously used to characterize the same PPARγ ligands (Berger et al., 2003; Thompson et al., 2004), we found that GAI scores were highly correlated with TA scores, the maximal ligand activation of PPARγ-GAL4 chimeric receptors transiently cotransfected into COS-1 cells with a pUAS(5X)-tk-luc reporter vector. In contrast, a still-significant but reduced correlation was seen between GAI scores and the maximal ligand-induced up-regulation of 3T3-L1 cell expression of the PPARγ target gene FABP4. We posit that the GAI is superior to both the TA and FABP4 expression scores. The GAI is derived from alterations in gene expression in 3T3-L1 adipocytes, which represent a more physiologically relevant cell system than the engineered COS-1 cells with which the TA score is derived. The GAI score is calculated from changes in the expression of numerous PPARγ-regulated genes in fully differentiated 3T3-L1 adipocytes, rather than the expression of only the FABP4 gene in undifferentiated 3T3-L1 cells. In addition, the correlations for GAI versus TA scores and GAI versus FABP4 scores were stronger than the correlation of TA versus FABP4 scores. Therefore, it is reasonable to conclude that determination of GAI scores should be more accurate for quantitative assessment of maximal PPARγ ligand activity, compared with the other two methods.

All TZD and non-TZD PPARγ full agonists had GAI scores of ~1.0, similar to that of the reference compound rosiglitazone. In contrast, SPPARγMs had a wide range of scores, from 0.2 to 0.82, whereas PPARα- and LXR-selective ligands had GAI scores of <0.1. Because the GAI scores were obtained from expression profiles obtained with saturating compound concentrations, we suggest that the magnitude of each compound's GAI score reflects the compound's intrinsic ability to activate PPARγ-mediated gene regulation maximally. The narrow range of GAI scores observed with PPARγ full agonists, compared with the wide range seen with SPPARγMs, and the marked gap between these score sets support the proposition that the molecular mechanisms through which these two ligand classes activate PPARγ are qualitatively different. It has been reported that TZD and non-TZD PPARγ full agonists, but not a variety of structurally distinct SPPARγMs, interact directly (through hydrogen bonding) with the Tyr473 residue within helix 12 of the receptor's LBD (Einstein et al., 2008). The binding of SPPARγMs differentially stabilizes regions of the PPARγ LBD other than helix 12 and generates receptor conformations of decreased stability, in comparison with PPARγ full agonists, which leads to the formation of distinct receptor-transcriptional coactivator complexes and reduced gene reg-

ulatory activity (Berger et al., 2003; Bruning et al., 2007). The broad continuous distribution of SPPARγM GAI scores coincides with the previously described allosteric mechanism of SPPARγM activation (Bruning et al., 2007), in which the extent of conformational change and stabilization of β-sheet and H3 regions within the receptor's LBD upon SPPARγM binding is flexible and continuous, spanning a wide dynamic range. Our studies support the observation that the expression of genes is fine-tuned, and not merely turned on and off, to meet the biological needs of cells (Meijsing et al., 2009). The maximal SPPARγM GAI score of 0.82 obtained in our studies closely coincides with the report that ligands demonstrating <80% transactivation efficacy versus rosiglitazone do not stabilize helix 12 and, therefore, a non–H12-dependent mechanism exists to control coactivator recruitment to the receptor in response to SPPARγMs (Bruning et al., 2007). Our results agree with previous observations that structurally distinct SPPARγMs can display a range of efficacious and adverse effects in rodent models of T2D (Doshi et al., 2010).

On the basis of the data described above, we hypothesized that the ideal PPARγ ligand would bind its receptor in a manner that would induce conformational changes favoring the formation of complexes with specific transcriptional cofactors that would optimize the regulation of target genes that control efficacy mechanisms while minimizing alterations in the expression of genes that mediate mechanism-based untoward effects. We found that SPPARγMs possess an important type of gene regulation selectivity. Specifically, we demonstrated that, in comparison with PPARγ full agonists, SPPARγMs could preferentially regulate to a greater extent a set of genes associated with antidiabetic efficacy in *db/db* mice, compared with a distinct gene set associated with the induction of cardiomegaly in SD rats. The genes selected for each of these two sets demonstrated changes in expression that correlated most closely with glucose level correction and cardiac hypertrophy endpoints, respectively. The greater alterations in the expression of antidiabetic efficacy-associated genes, relative to adverse effect-associated genes, by SPPARγMs concur with previous observations that SPPARγMs possess increased therapeutic windows, compared with PPARγ full agonists (Chang et al., 2008); the finding also agrees with the observation that SPPARγM signatures are dominated by genes involved in various metabolic pathways that might mediate their antidiabetic efficacy (Table 3). It is worth noting that the two gene sets described above are those that appear to be correlated most robustly with but are not necessarily causal to the observed antidiabetic efficacy and adverse effects. Relaxing selection thresholds and/or using other selection methods might produce more genes associated with SPPARγM selectivity. Given that our profiling experiments included seven PPARγ full agonists from both TZD and non-TZD structural classes and 70 SPPARγMs from multiple distinct structural classes, we think that the observed gene signatures and SPPARγM selectivity are not likely attributable to off-target, compound-specific effects. They almost certainly reflect the on-target, PPARγ-mediated effects produced by different PPARγ ligands.

Unlike maximal transcriptional activity quantified with the GAI, the SPPARγM selectivity we identified with the SI was independent of ligand dose. Maximal and selective transcriptional activities, as quantified with the GAI and the SI, respectively, describe different but complementary features of PPARγ ligand activity. PPARγ full agonists display high GAI scores but no measurable selectivity, whereas SPPARγMs display lower GAI scores and significant selectivity. Both GAI and SI scores can serve as important parameters for optimizing and selecting SPPARγMs for clinical development. We and others have long held the view that modulating PPARγ activity, rather than fully activating the receptor, would be the most effective strategy for treating T2D and associated metabolic disorders (Berger et al., 2003; Cock et al., 2004). As shown in our studies, PPARγ full agonists did not demonstrate selectivity in their regulation of antidiabetic efficacy- and adverse effect-associated genes over a wide dose range. It is reasonable to conclude that simply developing more-potent PPARγ full agonists would not lead to well tolerated therapeutic agents. In contrast, SPPARγMs are likely to yield efficacious antidiabetic drugs with superior tolerability. The SPPARγMs profiled here displayed consistently higher SI scores, compared with PPARγ full agonists, but the magnitude of these differences for the overwhelming majority of SPPARγMs assayed was ≤ 0.2 on a $\log_{10}$ scale, which indicates a maximal increase in expression of antidiabetic efficacy-associated genes versus adverse effect-associated genes of only 60%. We suggest that SPPARγMs with higher SI scores might be identified and such ligands would hold the promise of demonstrating greater therapeutic indices.

In summary, SPPARγMs produced attenuated gene signatures, relative to PPARγ full agonists, in both cultured 3T3-L1 adipocytes and rodent white adipose tissue. The gene signatures common to these two ligand classes encompassed a large proportion of the total SPPARγM signatures. These intersecting signatures were enriched in metabolic pathways that are likely to mediate many of the beneficial metabolic and insulin-sensitizing actions of all PPARγ ligands. Analysis of our extensive molecular profiling experiments revealed that SPPARγMs, unlike PPARγ full agonists, preferentially regulated an antidiabetic efficacy-associated gene set, in comparison with a distinct adverse effect-associated gene set. We also developed two novel, gene expression-based scores. The GAI quantifies a ligand's ability to stimulate maximal PPARγ transcriptional activity, whereas the SI quantifies a PPARγ ligand's induction of antidiabetic efficacy- versus adverse effect-associated genes and can differentiate SPPARγMs from PPARγ full agonists independent of dose. The studies described here have enhanced our understanding of SPPARγM actions on the transcriptome and provide a potential means to identify novel PPARγ ligands with comparable efficacy and superior tolerability, compared with currently available, PPARγ agonist, antidiabetic therapeutic agents.

Acknowledgments

We thank Merck Research Laboratory medicinal chemists for providing the SPPARγMs used in these studies. We express our gratitude to the Merck Gene Expression Laboratory for conducting the profiling experiments. We are indebted to Monica Einstein and Chuanlin Wang for performing PPARγ transactivation assays and to Ching Chang, Margaret Wu, and Margaret McCann for performing in vivo studies. We appreciate the support this project received from Nancy Thornberry. We are grateful to Guanghui Hu for critically reading and commenting on the manuscript.

Authorship Contributions

Participated in research design: Tan, Muise, Dai, Wong, Meinke, Lum, J. R. Thompson, and Berger.

Conducted experiments: Muise, Wong, G. M. Thompson, Wood, and Berger.

Contributed new reagents or analytic tools: G. M. Thompson, Wood, Meinke, and Lum.

Performed data analysis: Tan, Muise, Dai, Raubertas, Lum, and J. R. Thompson.

Wrote or contributed to the writing of the manuscript: Tan, Muise, Dai, Raubertas, Wong, Meinke, Lum, J. R. Thompson, and Berger.

References

Acton JJ 3rd, Akiyama TE, Chang CH, Colwell L, Debenham S, Doebber T, Einstein M, Liu K, McCann ME, Moller DE, et al. (2009) Discovery of (2*R*)-2-(3-{3-[(4-methoxyphenyl)carbonyl]-2-methyl-6-(trifluoromethoxy)-1*H*-indol-1-yl}phenoxy)butanoic acid (MK-0533): a novel selective peroxisome proliferator-activated receptor γ modulator for the treatment of type 2 diabetes mellitus with a reduced potential to increase plasma and extracellular fluid volume. *J Med Chem* **52:**3846–3854.

Acton JJ 3rd, Black RM, Jones AB, Moller DE, Colwell L, Doebber TW, Macnaul KL, Berger J, and Wood HB (2005) Benzoyl 2-methyl indoles as selective PPARgamma modulators. *Bioorg Med Chem Lett* **15:**357–362.

Berger J, Leibowitz MD, Doebber TW, Elbrecht A, Zhang B, Zhou G, Biswas C, Cullinan CA, Hayes NS, Li Y, et al. (1999) Novel PPARγ and PPARδ ligands produce distinct biological effects. *J Biol Chem* **274:**6718–6725.

Berger J and Moller DE (2002) The mechanisms of action of PPARs. *Annu Rev Med* **53:**409–435.

Berger JP, Petro AE, Macnaul KL, Kelly LJ, Zhang BB, Richards K, Elbrecht A, Johnson BA, Zhou G, Doebber TW, et al. (2003) Distinct properties and advantages of a novel peroxisome proliferator-activated protein γ selective modulator. *Mol Endocrinol* **17:**662–676.

Bruning JB, Chalmers MJ, Prasad S, Busby SA, Kamenecka TM, He Y, Nettles KW, and Griffin PR (2007) Partial agonists activate PPARγ using a helix 12 independent mechanism. *Structure* **15:**1258–1271.

Carley AN, Semeniuk LM, Shimoni Y, Aasum E, Larsen TS, Berger JP, and Severson DL (2004) Treatment of type 2 diabetic *db/db* mice with a novel PPARgamma agonist improves cardiac metabolism but not contractile function. *Am J Physiol Endocrinol Metab* **286:**E449–E455.

Center for Drug Evaluation and Research (2008) *Guidance for Industry: Diabetes Mellitus: Evaluating Cardiovascular Risk in New Antidiabetic Therapies to Treat Type 2 Diabetes*. Food and Drug Administration, Silver Spring, MD.

Chang CH, McNamara LA, Wu MS, Muise ES, Tan Y, Wood HB, Meinke PT, Thompson JR, Doebber TW, Berger JP, et al. (2008) A novel selective peroxisome proliferator-activator receptor-γ modulator – SPPARγM5 improves insulin sensitivity with diminished adverse cardiovascular effects. *Eur J Pharmacol* **584:**192–201.

Chen H, Charlat O, Tartaglia LA, Woolf EA, Weng X, Ellis SJ, Lakey ND, Culpepper J, Moore KJ, Breitbart RE, et al. (1996) Evidence that the diabetes gene encodes the leptin receptor: identification of a mutation in the leptin receptor gene in *db/db* mice. *Cell* **84:**491–495.

Combs TP, Wagner JA, Berger J, Doebber T, Wang WJ, Zhang BB, Tanen M, Berg AH, O'Rahilly S, Savage DB, et al. (2002) Induction of adipocyte complement-related protein of 30 kilodaltons by PPARgamma agonists: a potential mechanism of insulin sensitization. *Endocrinology* **143:**998–1007.

Cock TA, Houten SM, and Auwerx J (2004) Peroxisome proliferator-activated receptor-γ: too much of a good thing causes harm. *EMBO Rep* **5:**142–147.

Doshi LS, Brahma MK, Bahirat UA, Dixit AV, and Nemmani KV (2010) Discovery and development of selective PPARγ modulators as safe and effective antidiabetic agents. *Expert Opin Investig Drugs* **19:**489–512.

Einstein M, Akiyama TE, Castriota GA, Wang CF, McKeever B, Mosley RT, Becker JW, Moller DE, Meinke PT, Wood HB, et al. (2008) The differential interactions of peroxisome proliferator-activated receptor γ ligands with Tyr473 is a physical basis for their unique biological activities. *Mol Pharmacol* **73:**62–74.

Francis GA, Fayard E, Picard F, and Auwerx J (2003) Nuclear receptors and the control of metabolism. *Annu Rev Physiol* **65:**261–311.

Gerhold DL, Liu F, Jiang G, Li Z, Xu J, Lu M, Sachs JR, Bagchi A, Fridman A, Holder DJ, et al. (2002) Gene expression profile of adipocyte differentiation and its regulation by peroxisome proliferator-activated receptor-gamma agonists. *Endocrinology* **143:**2106–2118.

Hughes TR, Mao M, Jones AR, Burchard J, Marton MJ, Shannon KW, Lefkowitz SM, Ziman M, Schelter JM, Meyer MR, et al. (2001) Expression profiling using microarrays fabricated by an ink-jet oligonucleotide synthesizer. *Nat Biotechnol* **19:**342–347.

Institute of Laboratory Animal Resources (1996) *Guide for the Care and Use of Laboratory Animals* 7th ed. Institute of Laboratory Animal Resources, Commission on Life Sciences, National Research Council, Washington DC.

Kim MK, Chae YN, Kim HS, Choi SH, Son MH, Kim SH, Kim JK, Moon HS, Park SK, Shin YA, et al. (2009) PAR-1622 is a selective peroxisome proliferator-activated receptor gamma partial activator with preserved antidiabetic efficacy and broader safety profile for fluid retention. *Arch Pharm Res* **32:**721–727.

Knouff C and Auwerx J (2004) Peroxisome proliferator-activated receptor-gamma calls for activation in moderation: lessons from genetics and pharmacology. *Endocr Rev* **25:**899–918.

Larsen PJ, Lykkegaard K, Larsen LK, Fleckner J, Sauerberg P, Wassermann K, and Wulff EM (2008) Dissociation of antihyperglycaemic and adverse effects of partial perioxisome proliferator-activated receptor (PPAR-gamma) agonist balaglitazone. *Eur J Pharmacol* **596:**173–179.

Liu K, Black RM, Acton JJ 3rd, Mosley R, Debenham S, Abola R, Yang M, Tschirret-Guth R, Colwell L, Liu C, et al. (2005) Selective PPARgamma modulators with improved pharmacological profiles. *Bioorg Med Chem Lett* **15:**2437–2440.

Meijsing SH, Pufall MA, So AY, Bates DL, Chen L, and Yamamoto KR (2009) DNA binding site sequence directs glucocorticoid receptor structure and activity. *Science* **324:**407–410.

Motani A, Wang Z, Weiszmann J, McGee LR, Lee G, Liu Q, Staunton J, Fang Z, Fuentes H, Lindstrom M, et al. (2009) INT131: a selective modulator of PPAR gamma. *J Mol Biol* **386:**1301–1311.

Peraza MA, Burdick AD, Marin HE, Gonzalez FJ, and Peters JM (2006) The toxicology of ligands for peroxisome proliferator-activated receptors (PPAR). *Toxicol Sci* **90:**269–295.

Rangwala SM and Lazar MA (2004) Peroxisome proliferator-activated receptor gamma in diabetes and metabolism. *Trends Pharmacol Sci* **25:**331–336.

Saltiel AR and Olefsky JM (1996) Thiazolidinediones in the treatment of insulin resistance and type II diabetes. *Diabetes* **45:**1661–1669.

Schoonjans K, Staels B, and Auwerx J (1996) Role of the peroxisome proliferator-activated receptor (PPAR) in mediating the effects of fibrates and fatty acids on gene expression. *J Lipid Res* **37:**907–925.

Sohn KA, Cruciani-Guglielmacci C, Kassis N, Clément L, Ouali F, Caüzac M, Lebègue N, Berthelot P, Caignard DH, Pégorier JP, et al. (2009) S26948, a new specific peroxisome proliferator activated receptor gamma modulator improved in vivo hepatic insulin sensitivity in 48 h lipid infused rats. *Eur J Pharmacol* **608:**104–111.

Thompson GM, Trainor D, Biswas C, LaCerte C, Berger JP, and Kelly LJ (2004) A high-capacity assay for PPARgamma ligand regulation of endogenous aP2 expression in 3T3–L1 cells. *Anal Biochem* **330:**21–28.

Tontonoz P, Hu E, and Spiegelman BM (1994) Stimulation of adipogenesis in fibroblasts by PPAR gamma 2, a lipid-activated transcription factor. *Cell* **79:**1147–1156.

Wang M and Tafuri S (2003) Modulation of PPARgamma activity with pharmaceutical agents: treatment of insulin resistance and atherosclerosis. *J Cell Biochem* **89:**38–47.

Weng L, Dai H, Zhan Y, He Y, Stepaniants SB, and Bassett DE (2006) Rosetta error model for gene expression analysis. *Bioinformatics* **22:**1111–1121.

Willson TM, Lambert MH, and Kliewer SA (2001) Peroxisome proliferator-activated receptor gamma and metabolic disease. *Annu Rev Biochem* **70:**341–367.

Zhang F, Lavan BE, and Gregoire FM (2007) Selective modulators of PPAR-γ activity: molecular aspects related to obesity and side-effects. *PPAR Res* **2007:** 32696.

Address correspondence to: Dr. John R. Thompson, Merck Research Laboratories, P.O. Box 2000, Rahway, NJ 07065. E-mail: john_thompson@merck.com